

Supporting Information

Label-Free, Single Protein Detection on a Near Infrared Fluorescent Single-Walled Carbon Nanotube/Protein Microarray Fabricated by Cell-Free Synthesis

Jin-Ho Ahn[†], Jong-Ho Kim[†], Nigel F. Reuel, Paul W. Barone, Ardemis A. Boghossian, Jingqing Zhang, Hyeonseok Yoon, Alice C. Chang, Andrew J. Hilmer, Michael S. Strano^{*}

Department of Chemical Engineering, Massachusetts Institute of Technology, Cambridge, MA 02139, USA

[†] These authors equally contributed to this work.

^{*} To whom correspondence should be addressed. Email: strano@mit.edu

This PDF file includes:

Materials and Methods

Supporting Table S1. Oligonucleotide primers used in this study.

Supporting Fig. S1: Functionalization of SWNT/CHI array with Ni-NTA.

Supporting Fig. S2: Deconvolution of nIR fluorescence of SWNTs in response to His-tag protein (Ack) in SWNT/CHI array.

Supporting Fig. S3: Generation of expression template by PCR.

Supporting Fig. S4: Investigation of reproducibility on SWNT/CHI protein array with various control experiments.

Supporting Fig. S5: Selective recognition of protein-protein interactions on SWNT/CHI array.

Supporting Fig. S6: Western blot analysis.

Supporting Fig. S7: Single molecule detection of protein-protein interaction on SWNT/CHI microarray.

Supporting Fig. S8: Protein-protein interactions on SWNT/CHI array.

Supporting Fig. S9: Distance calculation between the SWNT and Ni-NTA moiety.

Supporting Fig. S10: Published literature of protein-protein interaction shown in Figure 5b.

Supporting Fig. S11: Homo-multimer interaction analysis based on literature survey.

Materials

ATP, GTP, UTP, CTP, creatine phosphate, creatine kinase and the *E. coli* total tRNA mixture were purchased from Roche Applied Science (Indianapolis, IN). All the other reagents for cell-free system were purchased from Sigma (St. Louis, MO). The *E. coli* strain BL21-StarTM(DE3) was purchased from Invitrogen (Carlsbad, CA). Acetic acid, chitosan, succinic anhydride, *N,N*-diisopropylethylamine (DIEA), *N,N*-dimethylformamide (DMF), *N*-(3-dimethylaminopropyl)-*N'*-ethylcarbodiimide hydrochloride (EDC·HCl), *N*-hydroxysuccinimide (NHS), *Nα,Nα*-bis(carboxymethyl)-L-lysine (NTA), nickel (II) sulfate and glutaraldehyde solution (50 vol%) were purchased from Sigma-Aldrich. The patterned glass functionalized with poly-L-lysine was purchased from Tekdon Inc. Single-walled carbon nanotubes were purchased from Nano-C Inc.

Preparation of cell extract

The S30 cell extracts were prepared from *E. coli* strain BL21 StarTM(DE3) (Novagen, Madison, WI) according to the method reported elsewhere¹⁻³. The cells were grown at 37 °C in 4 L of 2xYT medium with agitation and aeration. When the cell density (OD₆₀₀) reached 0.5, isopropyl-thiogalactopyranoside (IPTG, 0.5 mM) was added to the culture media to induce T7 RNA polymerase expression. The cells were harvested when the OD₆₀₀ reached 4.0 and cells were washed three times by suspending them in 20 mL of S30 buffer per gram of wet cells and then centrifuged. S30 buffer contained 10 mM Tris–acetate buffer (pH 8.2), 14 mM magnesium acetate, 60 mM potassium glutamate, and 1 mM dithiothreitol (DTT) containing 0.05% (v/v) 2-mercaptoethanol (2-ME). The resulting cell pellets were weighed and then suspended with 12.7 mL of S30 buffer without 2-ME and disrupted in a French press cell (Thermo Scientific) at a constant pressure of 20,000 psi. The crude lysate was then centrifuged at 12,000 RCF for 10 min,

and the recovered supernatant was briefly incubated at 37 °C. The resulting extract was divided into small aliquots and stored at −80 °C before use for cell-free expression.

Gene preparation

Target ORFs were amplified using primers P1s and P2s. The first PCR products were purified by gel extraction and used for the second-round PCR, in which the full expression templates were synthesized using the P3 and P4 (**Supporting Fig. 3**). Primer sequences are listed in **Supporting Table 1**. After amplification, the final PCR products were used in cell-free protein synthesis reaction without purification³.

Spectroscopy and microscopy

Near-infrared photoluminescence spectra were acquired using 785 nm excitation and an Acton SP-500 spectrograph coupled to a Princeton instruments OMA V InGaAs detector. Absorption measurements were taken with a Shimadzu UV-3101 PC UV-VIS-NIR scanning spectrophotometer.

Microscopy and Data Analysis for Single Molecule Detection of Protein

After SWNT/CHI film was functionalized with Ni-NTA, the nIR fluorescence response of SWNT to His-tag EGFP as a capture protein and anti-His-tag antibody as a analyte was imaged and monitored in real-time for 25 min through a 100x TIRF objective using an inverted microscope (Carl Zeiss, Axiovert 200) attached with a 2D InGaAs array (Princeton Instruments OMA 2D) with a 658 nm laser excitation (LDM-OPT-A6-13, Newport Corp., 35 mW). The nIR fluorescence response movies were acquired at 1.0 sec/frame using the WinSpec data acquisition

program (Princeton Instruments). Before the experiment, a control movie was taken for 25 min to ensure a stable baseline. A 20 μ L portion of His-tag EGFP (final concentration: 100 μ g/ml) was added into the SWNT/CHI film bearing Ni-NTA 5 min after taking the movie in PBS (pH 7.4, 10 mM) without addition of proteins, and the fluorescence response was further imaged and monitored for 10 min. Then, a 10 μ L portion of anti-His-tag antibody (final concentration: 23 μ g/ml) was added into EGFP-immobilized SWNT/CHI film, and the fluorescence response was monitored for 10 min. The fluorescence response within a 2×2 pixel spatial binning region in the movie images was examined, and the analysis algorithm is similar to that reported before⁴. The four-pixel area in the image corresponds to a 600×600 nm² region in the real sample, representing the PL from a single SWNT, which is determined by the diffraction limit in the nIR range⁵. Hidden Markov Modeling (HMM) is employed to correlate the rate constants of immobilization of His-tag EGFP to Ni-NTA and binding of anti-His-tag antibody to EGFP on the SWNT/CHI film.

Sensitivity of SWNT/CHI microarray to protein detection

A 40 μ L of His-tag EGFP (initial concentration; 5 mg/mL) was added to SWNT/CHI microarray bearing Ni²⁺ in 1 mL of PBS (pH 7.4, 10 mM), and then incubated for 30 min at room temperature. After washing out the unbound His-tag EGFP with PBS, the SWNT/CHI bearing His-tag EGFP in 1 mL of PBS was placed on the nIR fluorescence microscope (100x objective, 658 nm laser) to focus on the array of single SWNT. The 15 μ L of the serially-diluted analyte protein from 100 nM to 10 pM (anti-His-tag antibody, initial concentration; 1 mg/mL) was added to the SWNT/CHI microarray in 1 mL of PBS 100 sec after taking the fluorescence image of

SWNT without addition of the analyte protein. The fluorescence response was further measured for 20 min at room temperature, and the collected movie was then analyzed as described above.

Control experiments

Various control experiments including negative and positive controls were performed (**Supporting Fig. 4**). Each reagent as positive or negative controls was added to each array wells in a humidified chamber at 37°C and incubated for 2 h. The fluorescence response of each SWNT/CHI well was measured. The arrays were washed three times for 10 min each with PBS buffer (pH 7.4, 10 mM) at RT and then PL spectra were taken. As shown in Supporting Figure 4, all reagents and buffers that are used as components in cell-free reaction mixture were tested and DNA expression templates including no ribosome binding site and no His-tag were also tested as negative control. On the other hand, His-tag coding expression templates, Fos, Jun, EGFP were tested as positive controls. Only His-tag containing proteins cause fluorescence decrease. Hence, the capture proteins are effectively and selectively expressed by cell-free synthesis on each spot of the array and no fluorescence decrease induced from other reagents in a cell-free protein expression system was detected.

References for Supporting Information

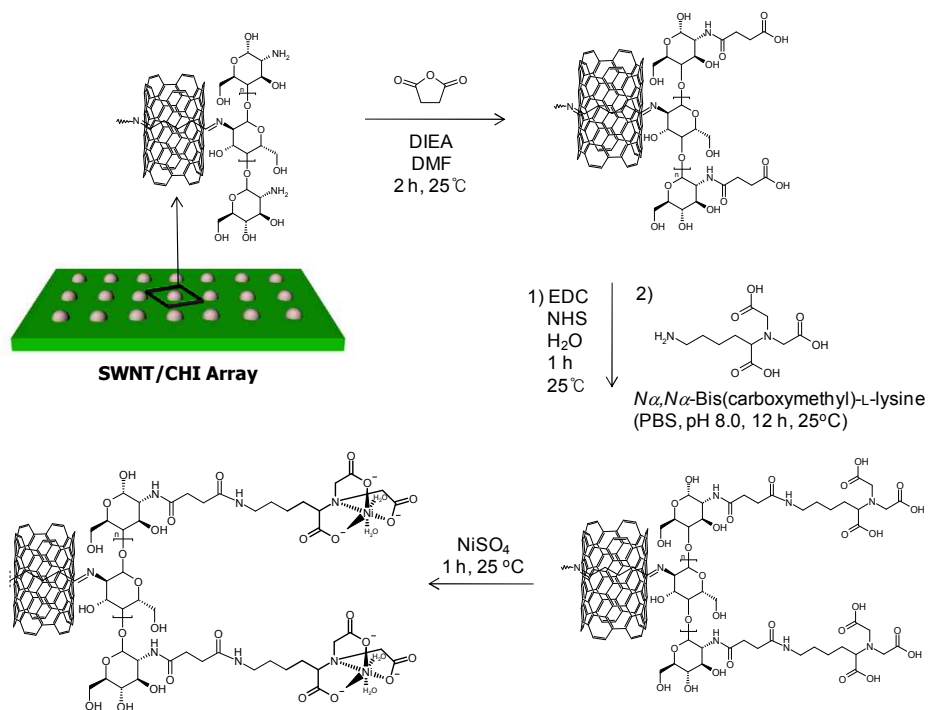
1. Kim, T.W., Oh, I.S., Ahn, J.H., Choi, C.Y. & Kim, D.M. Cell-free synthesis and in situ isolation of recombinant proteins. *Protein Expres Purif* **45**, 249-254 (2006).
2. Ahn, J.H. et al. Cell-free synthesis of recombinant proteins from PCR-amplified genes at a comparable productivity to that of plasmid-based reactions. *Biochem Bioph Res Co* **338**, 1346-1352 (2005).
3. Ahn, J.H., Keum, J.W. & Kim, D.M. High-throughput, combinatorial engineering of initial codons for tunable expression of recombinant proteins. *J Proteome Res* **7**, 2107-2113 (2008).
4. Jin, H., Heller, D.A., Kim, J.H. & Strano, M.S. Stochastic Analysis of Stepwise Fluorescence Quenching Reactions on Single-Walled Carbon Nanotubes: Single Molecule Sensors. *Nano Letters* **8**, 4299-4304 (2008).

5. Cognet, L. et al. Stepwise quenching of exciton fluorescence in carbon nanotubes by single-molecule reactions. *Science* **316**, 1465-1468 (2007).

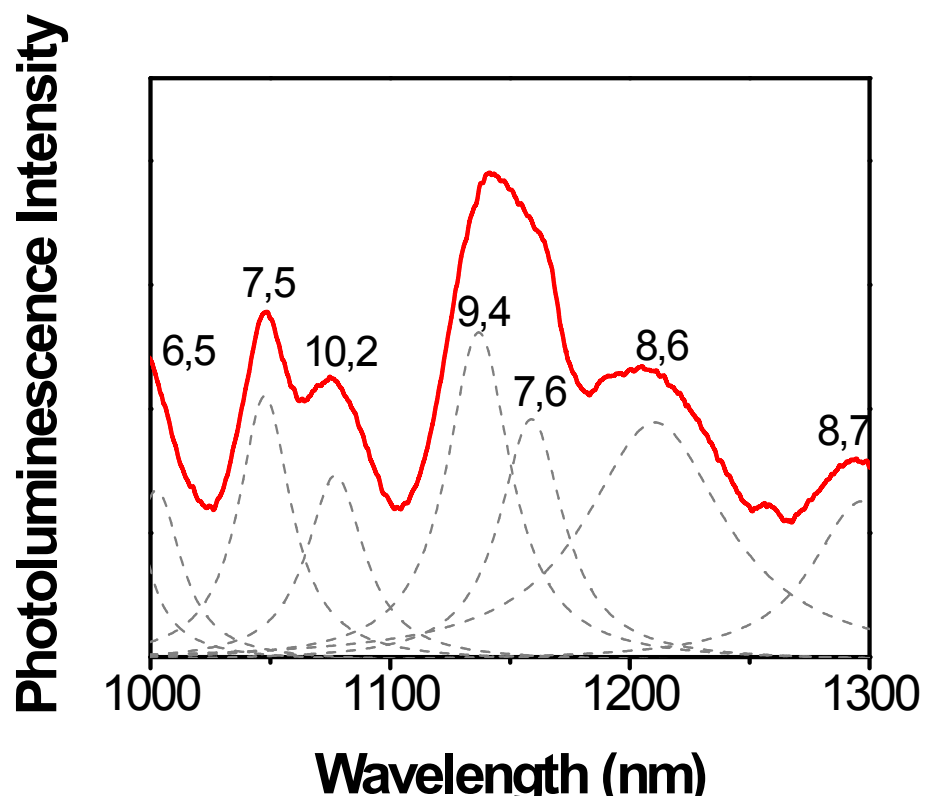
Supporting Table 1. Oligonucleotide primers used in this study.

Protein^a	P1	P2
Ack (P0A6A3)	aagaaggagatatacatatgtcagtaagtttagtactggt	ttaatgatgatgatgatgatgggcagtcaggcggctcgcgt
Dnak (P0A6Y8)	aagaaggagatatacatatgggtaaaataattggtatcga	ttaatgatgatgatgatgatgtttttgtctttgacttctt
FbaA (P0AB71)	aagaaggagatatacatatgtctaagattttgatttcgt	ttaatgatgatgatgatgatgcagaacgtcagtcgcgttca
GlyA (P0A825)	aagaaggagatatacatatgttaaagcgtgaaatgaacat	ttaatgatgatgatgatgatgtgcgtaaacgggtaacgtg
LpdA (P0A9P0)	aagaaggagatatacatatgagtactgaaatcaaaactca	ttaatgatgatgatgatgatgcttcttctcgtttcgggt
RpoA (P0A7Z4)	aagaaggagatatacatatgcagggttctgtgacagagtt	ttaatgatgatgatgatgatgctcgtcagcgatgcttgccg
RplB (P60422)	aagaaggagatatacatatggcagttgttaaatgtaaacc	ttaatgatgatgatgatgatgtttgctacggcgacgtacga
RpsB (P0A7V0)	aagaaggagatatacatatggcaactgtttccatgcgcga	ttaatgatgatgatgatgatgctcagcttctacgaagcttt
Tsf (P0A6P1)	aagaaggagatatacatatggctgaaattaccgcatcct	ttaatgatgatgatgatgatgagactgcttgacatcgcag
Ada (P06134)	aagaaggagatatacatatgaaaaagccacatgcttaac	ttaatgatgatgatgatgatgcctctcctcattttcagctt
Cdd (P0ABF6)	aagaaggagatatacatatgcatccacgttttcaaaccgc	ttaatgatgatgatgatgatgagcgagaagcactcggtcga
CDK4 (P11802)	aagaaggagatatacatatggctacctctcgatatga	ttaatgatgatgatgatgatgcaactccggattaccttcat
p16 (P42771)	aagaaggagatatacatatggtgcgcaggttcttggt	atgatgatgatgatgatgttacaactccggattaccttcat (noHis)
Jun (P05412)	aagaaggagatatacatatgactgcaagatggaaac	ttaatgatgatgatgatgatgcaagccaggtccacgggcag
Fos (P01100)	aagaaggagatatacatatgatgttctcgggctcaa	atgatgatgatgatgatgttacaagccaggtccacgggcag (noHis)
		ttaatgatgatgatgatgatgggtcaaatgtttgcaactgct
		atgatgatgatgatgatgttagtcaaatgtttgcaactgct (noHis)
		ttaatgatgatgatgatgatgcaacagggccagcagcgtgg
		atgatgatgatgatgatgttacaacagggccagcagcgtgg (noHis)
P3: Mega-F	TCGATCCCGCGAAATTAATACGACTCACTATAGGGAGACCACAACGGTTTCCCTCTAGAAAT AATTTTGTTTAACTTTAAGAAGGAGATATACATATG	
P4: Mega-R	CAAAAAACCCCTCAAGACCCGTTTAGAGGCCCAAGGGTTATGCTAGCTCGAGAAGCTTG TCGACGAATTCGGATCCTTAATGATGATGATGATGATG	

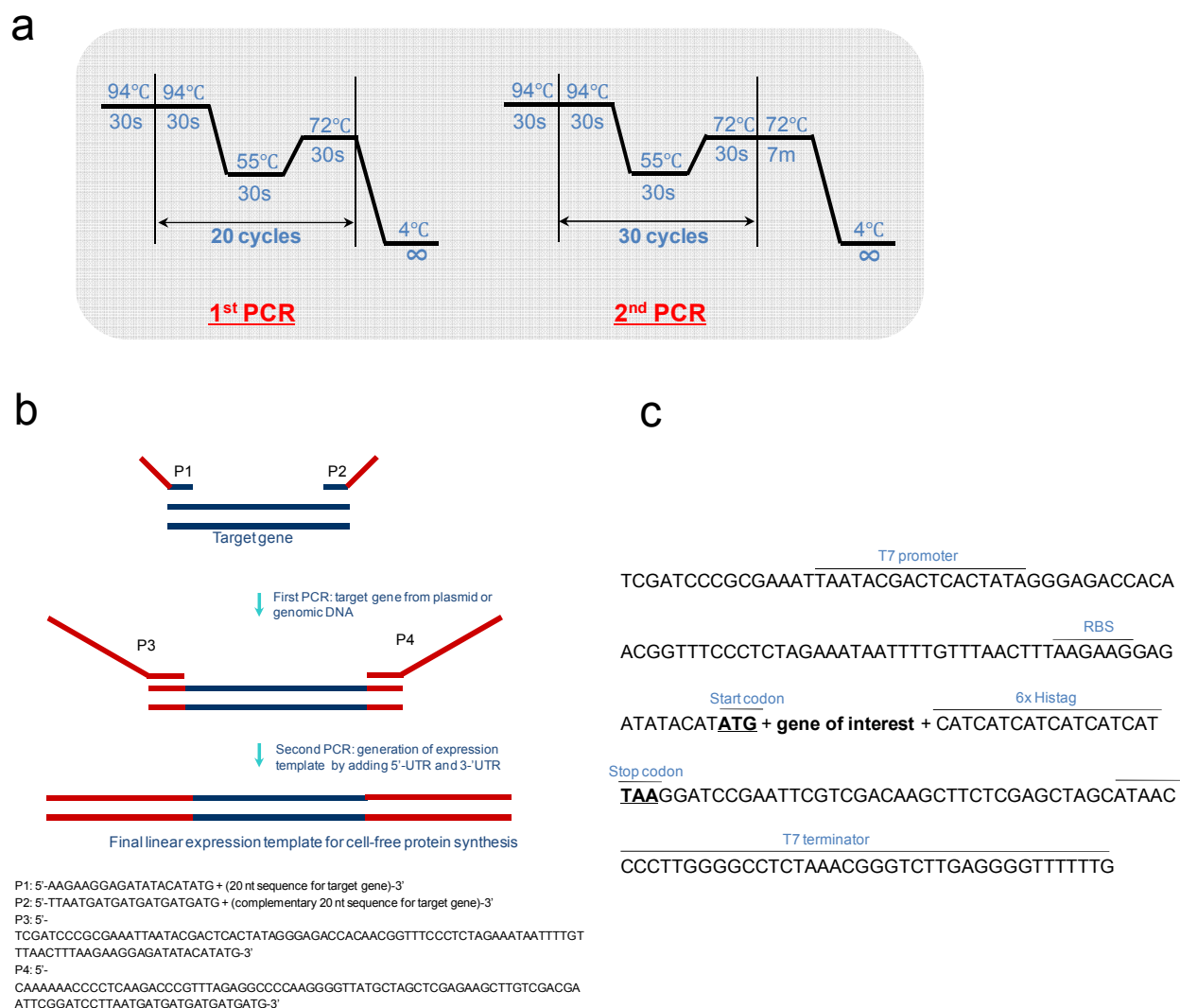
^aExPASy accession ID in parenthesis



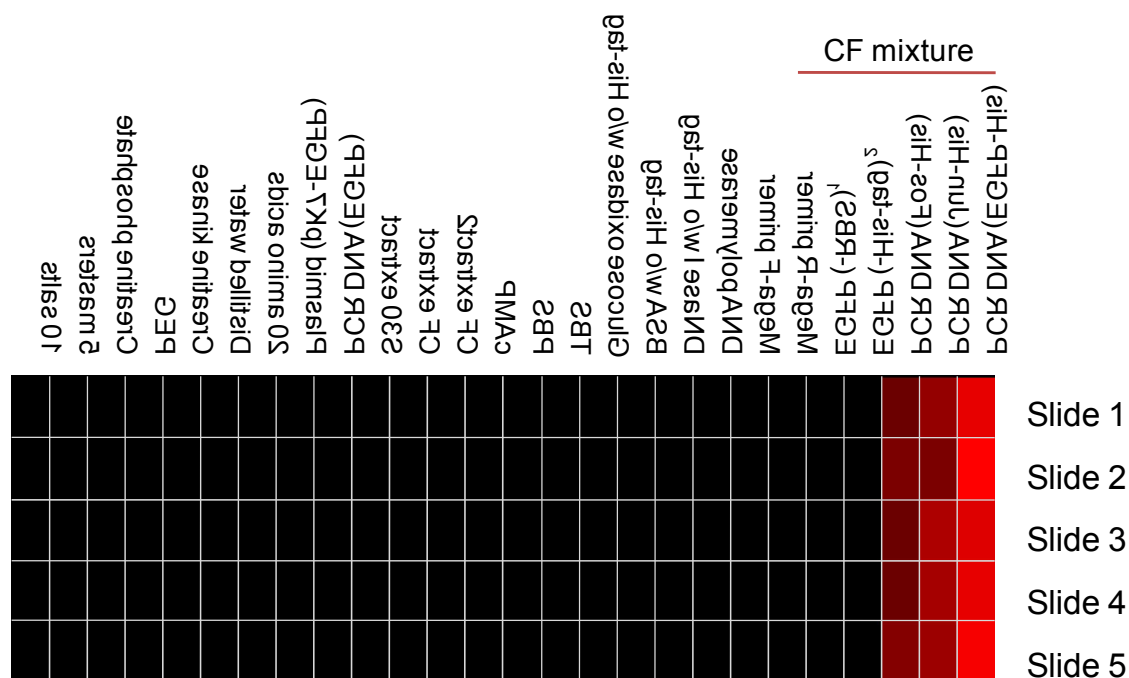
Supporting Figure S1. Functionalization of SWNT/CHI array with Ni-NTA.



Supporting Figure S2. Deconvolution of nIR fluorescence of SWNTs in response to His-tag protein (Ack) in SWNT/CHI array.



Supporting Figure S3. Generation of expression template by PCR. (a) Conditions for two-step PCR. (b) Two-step PCR, the gene of interest is amplified in the primary PCR via specific primers that are introducing an overlap region (primers P1 and P2). In a second PCR, the outer primers P3 and P4 bind to the overlapping region and add all regulatory elements necessary for transcription and translation. (c) Nucleotide sequence of amplified linear expression template for cell-free protein expression.

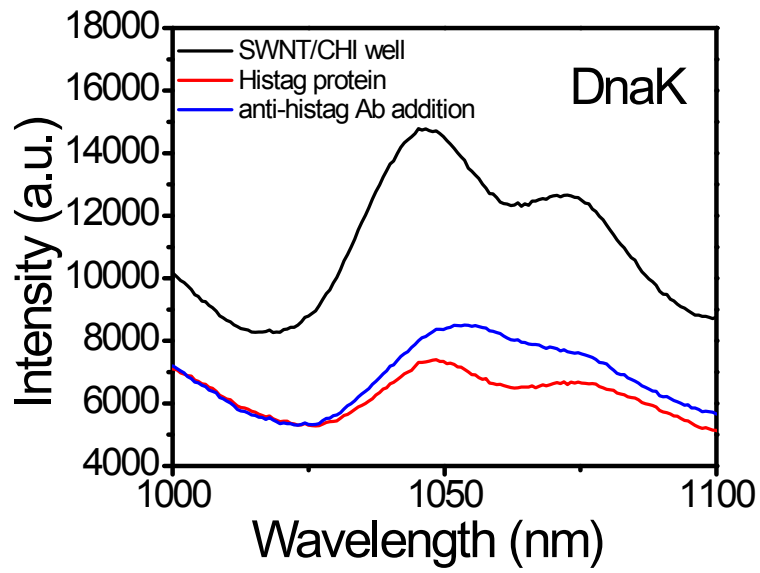


¹EGFP(-RBS): only transcription
TCGATCCCGCGAAATTAATACGACTCACTATAGGGAGACCACAACGGTTTCCCTCTAGAAATAATTTTGTTAACTTTA
AGUUCUCATATACCATG-

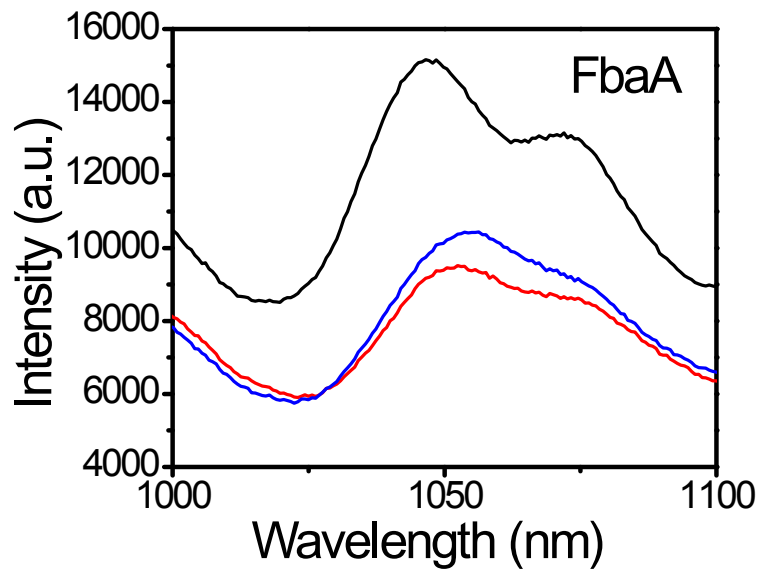
²EGFP(-stop): no His-tag
TAACATCATCATCATCATTAAGGATCCGAATTCGTCGACAAGCTTCTCGAGCTAGCATAACCCCTTGGGGCCTC
TAAACGGGCTTGAGGGGTTTTTTG

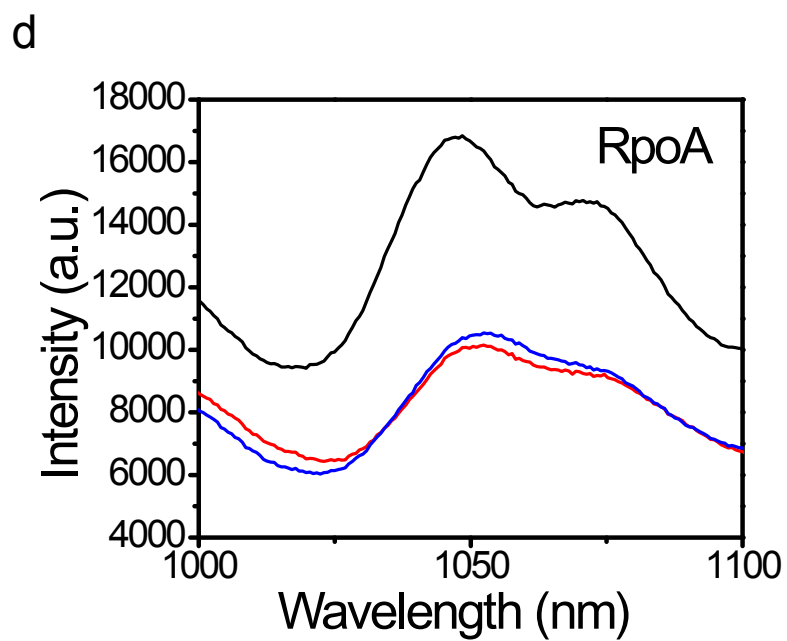
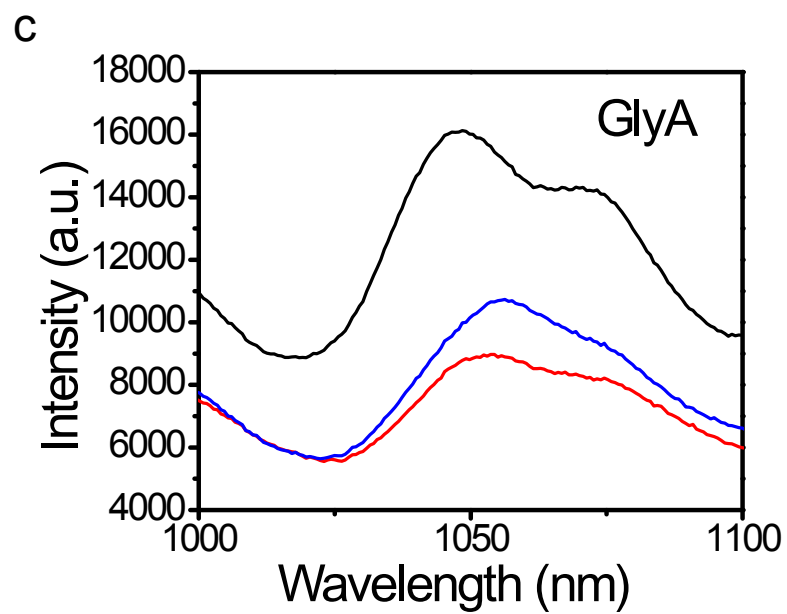
Supporting Figure S4. Investigation of reproducibility on SWNT/CHI protein array with various control experiments. All reagents and buffers used in cell-free reaction mixture were tested and DNA expression templates including no ribosome binding site and no His-tag were also tested as negative control. Each reagent indicated above as positive or negative controls was added to each array wells in a humidified chamber at 37°C and incubated for 2 h. The fluorescence response of each SWNT/CHI well was measured. The arrays were washed three times for 10 min each with PBS buffer (pH 7.4, 100 mM) at RT and then PL spectra were taken. 10 salts (90 mM of potassium glutamate, 80 mM of ammonium acetate, 12 mM of magnesium acetate); 5 masters (57 mM of Hepes-KOH (pH 8.2), 1.2 mM of ATP, 0.85 mM each of CTP, GTP and UTP, 0.64 mM of cAMP, 34 µg/ml of L-5-formyl-5,6,7,8-tetrahydrofolic acid (folinic acid), 1 mM each of 20 amino acids, 0.17 mg/ml of *E. coli* total tRNA mixture (from strain MRE600)); CF extract (cell-free reaction mixture w/o expressible DNAs).

a

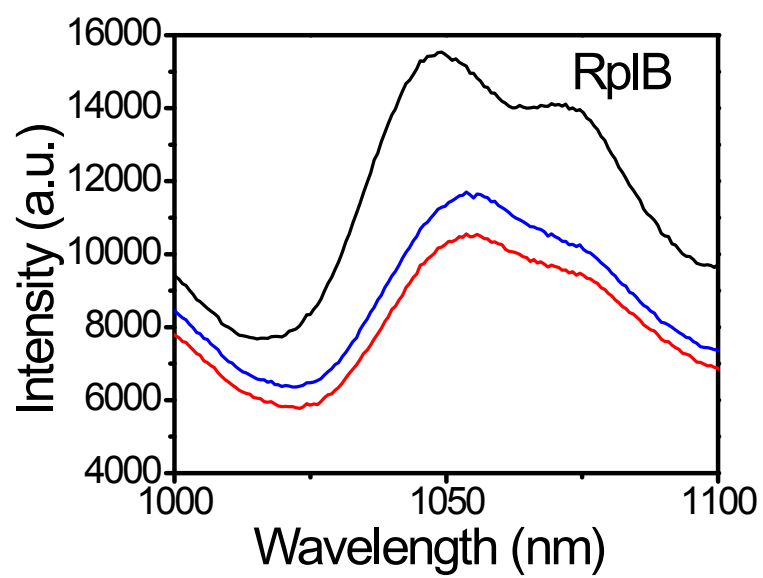


b

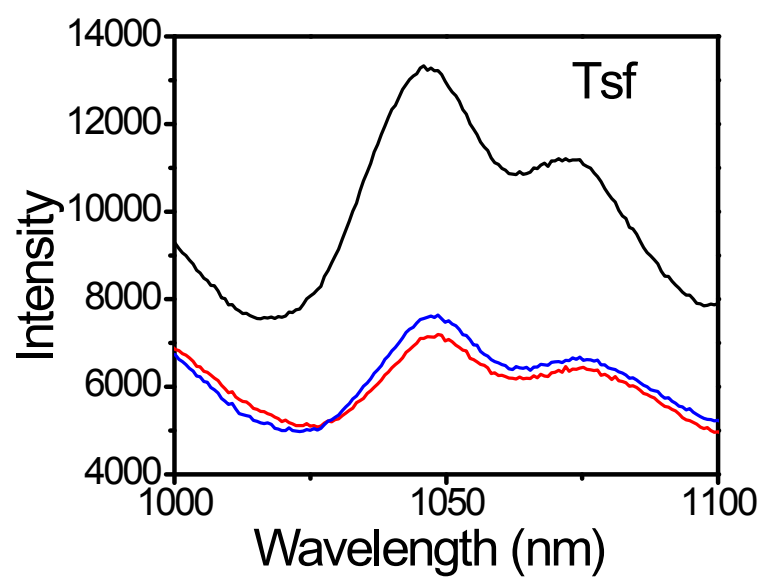




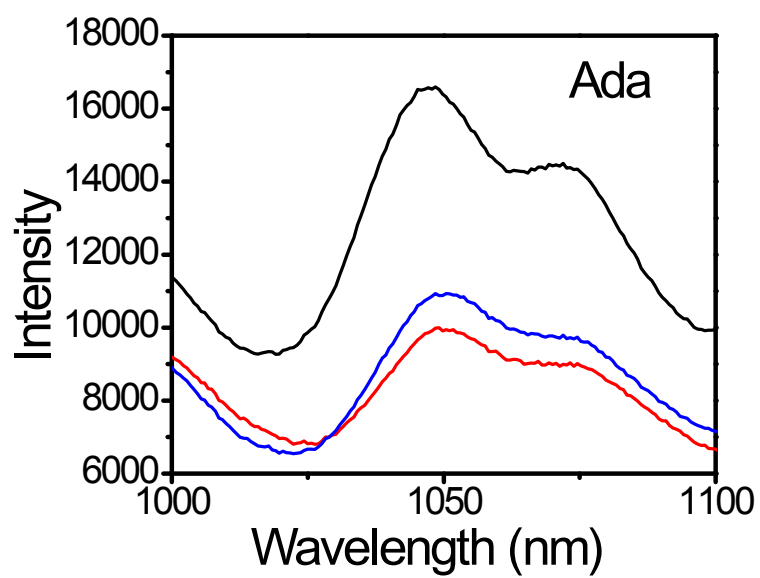
e



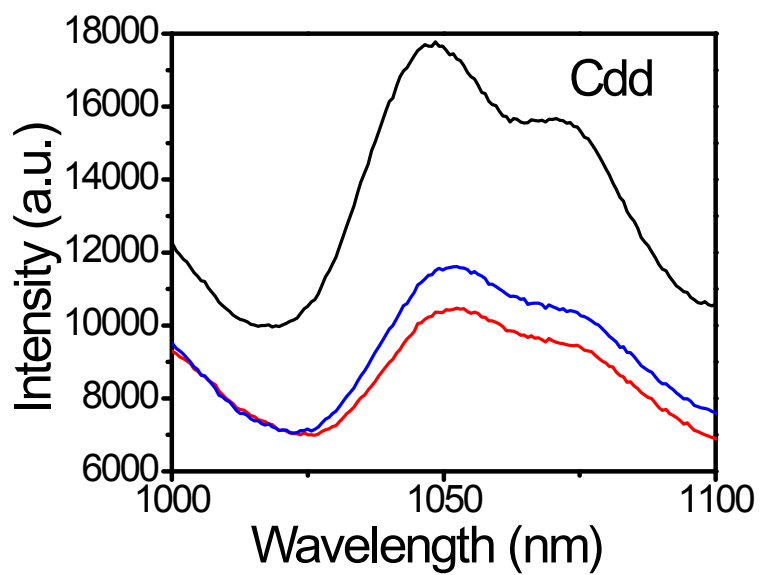
f



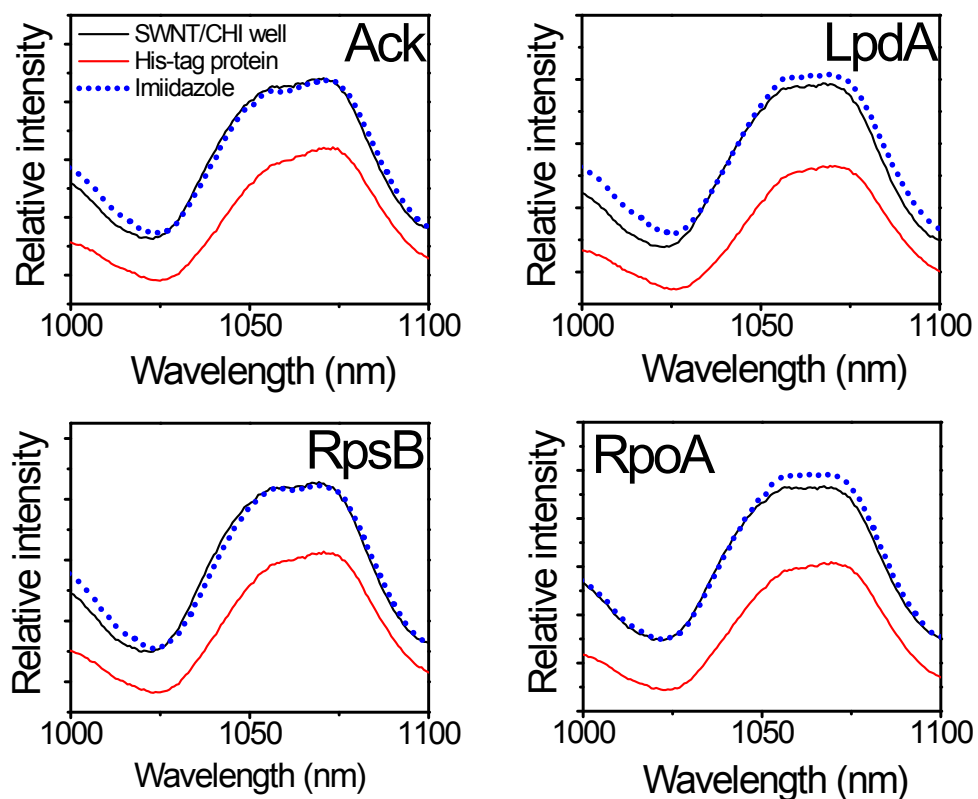
g



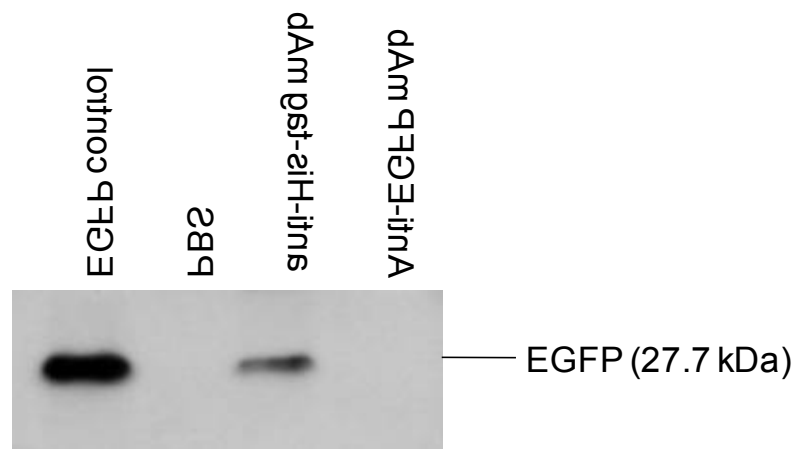
h



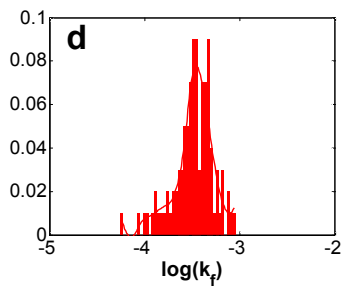
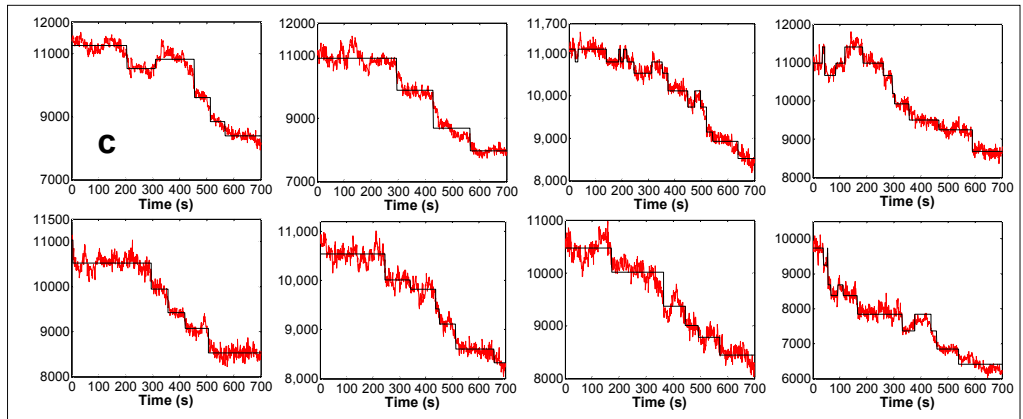
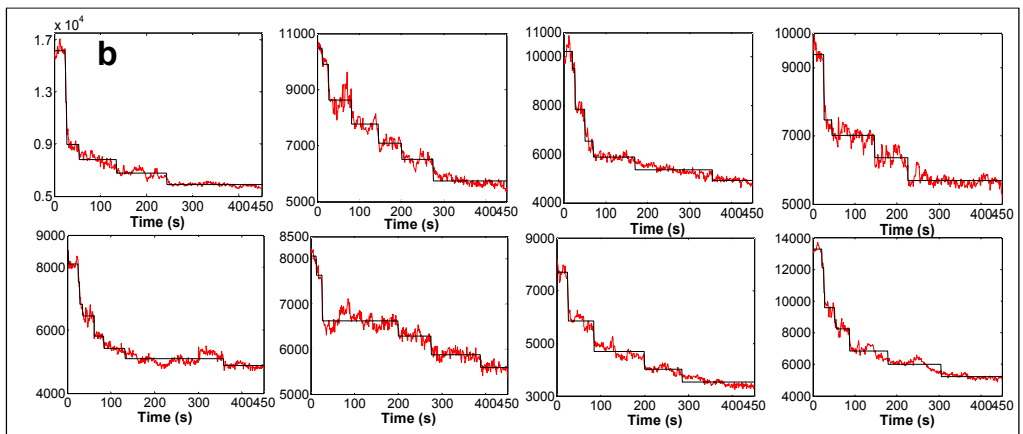
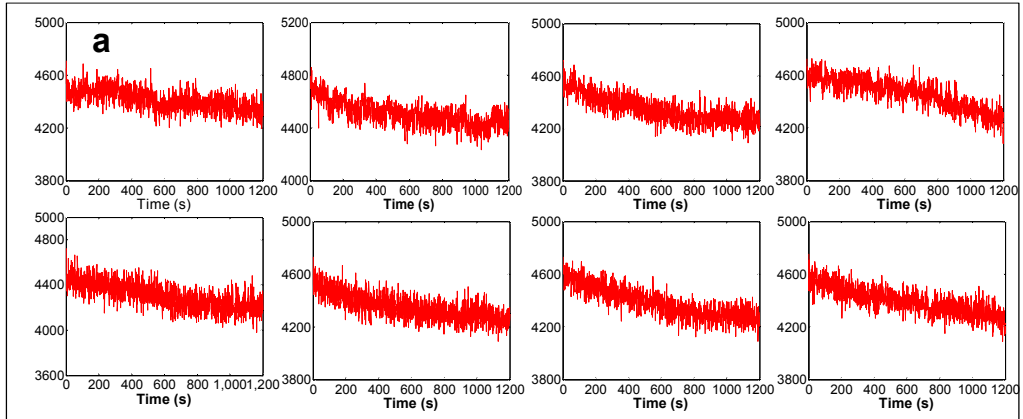
i

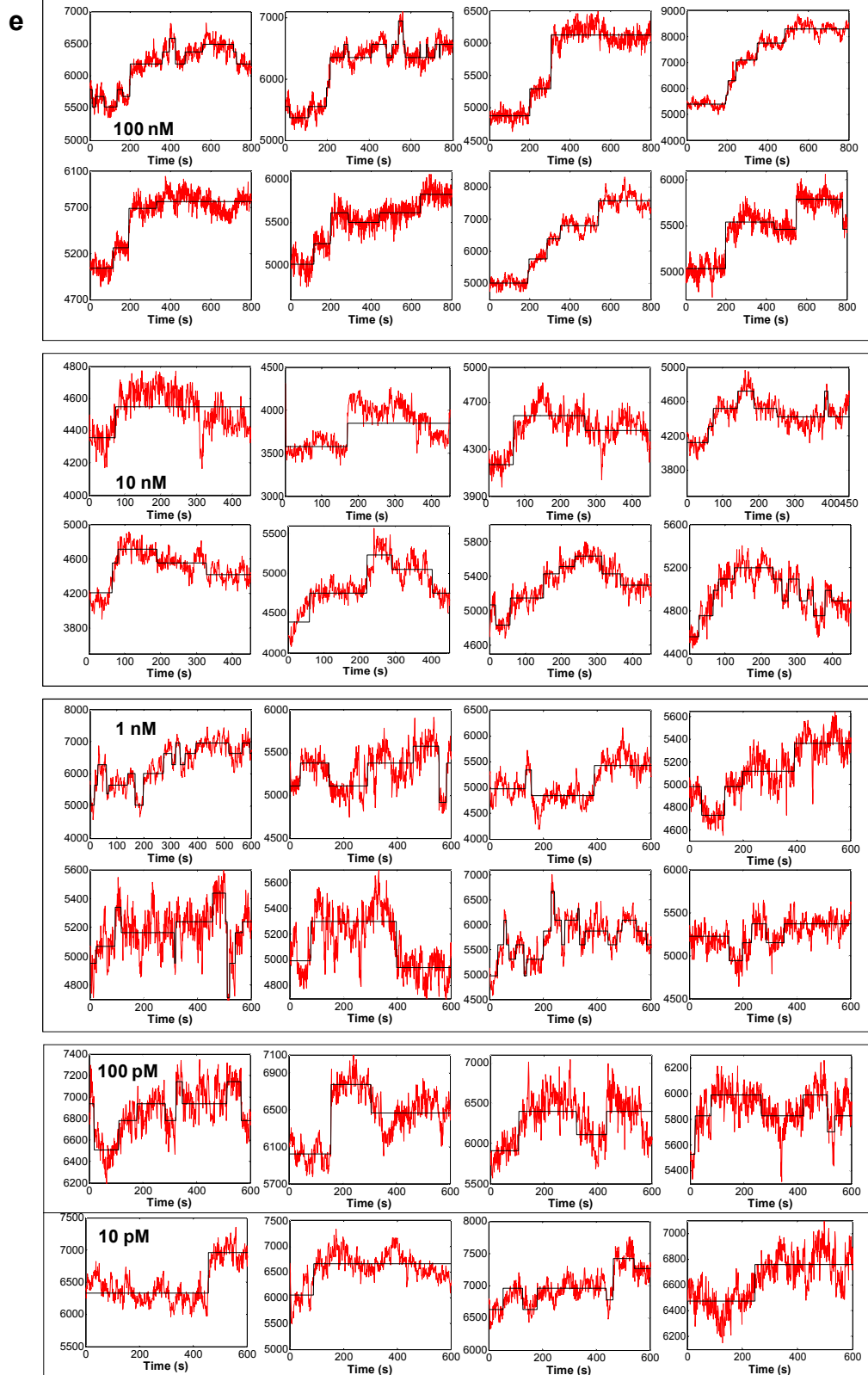


Supporting Figure S5. Selective recognition of protein-protein interactions on SWNT/CHI array. nIR fluorescence response of SWNT to protein immobilization and interaction with anti-His-tag antibody, showing fluorescence diminution for immobilization of His-tag proteins and increase for binding anti-His-tag antibody (a-h). (i) Imidazole addition: demonstration of protein binding reversibility on the SWNT/CHI array; quenched fluorescence is completely restored after treatment with an imidazole elution buffer (250 mM).

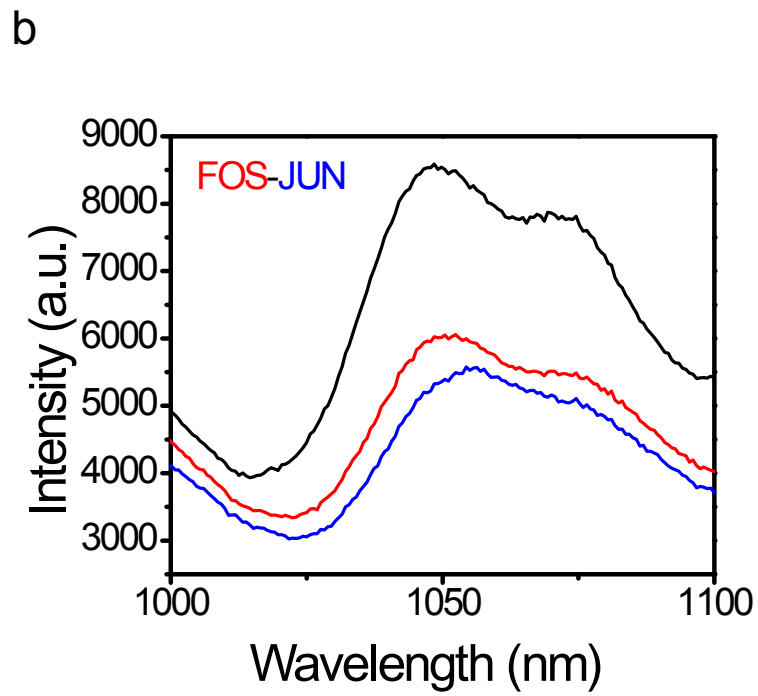
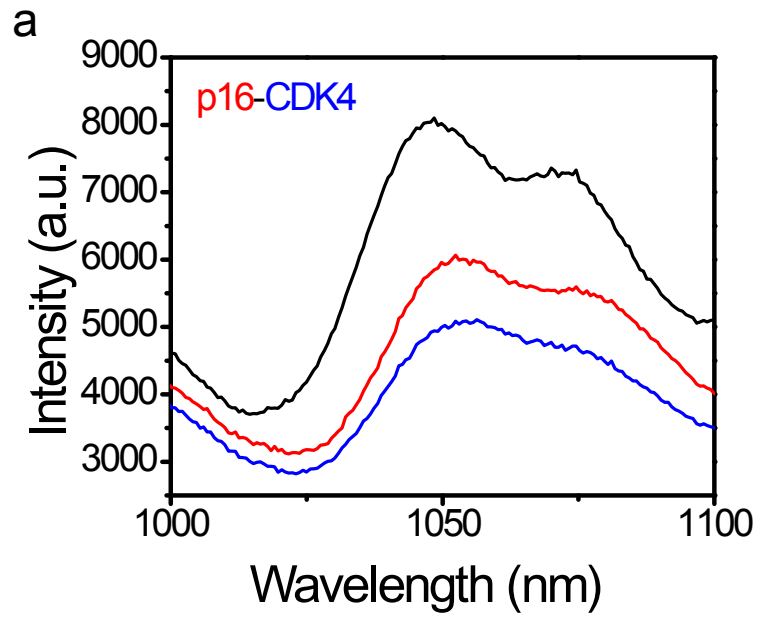


Supporting Figure S6. Western blot analysis. After incubation of His-tagged EGFP, each well was treated with monoclonal anti-His-tag antibody and anti-EGFP antibody for 30 min, and the eluted fractions were analyzed by 15% SDS-PAGE/Western blot using the monoclonal anti-His-tag antibody to detect EGFP protein.

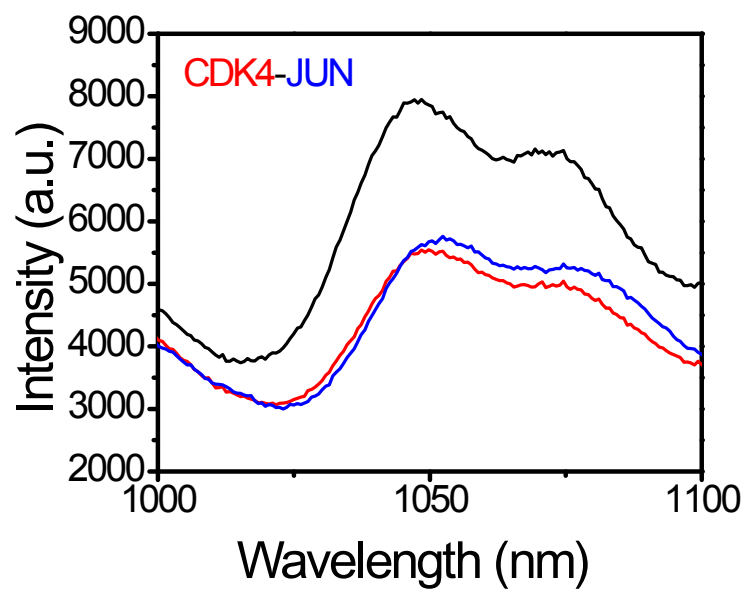




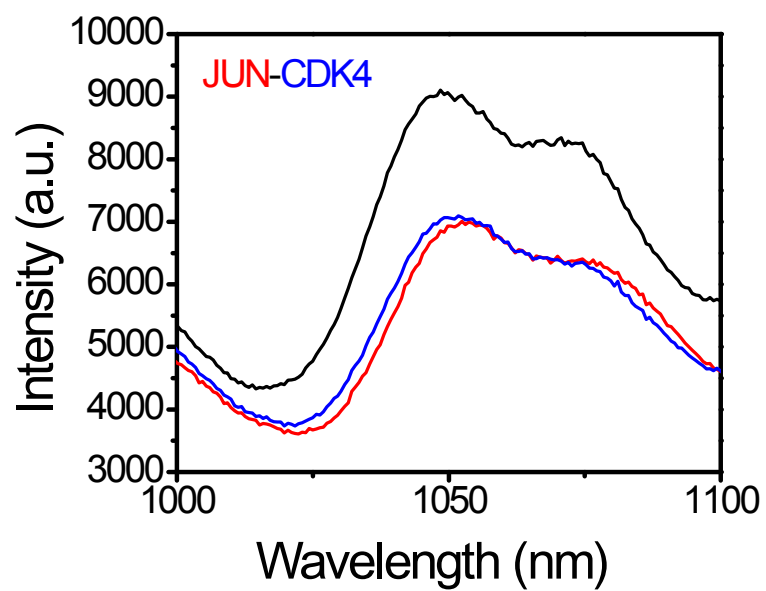
Supporting Figure S7. Single molecule detection of protein-protein interaction on SWNT/CHI microarray. (a) Representative fluorescence time-traces (red) without protein addition as a control, showing that SWNT emission is stable with zero mean deflection. (b) Representative fluorescence time-traces (red) for addition of Ni^{2+} to the NTA-bearing SWNT/CHI spot, showing stepwise quenching response. (c) Representative fluorescence time-traces (red) for the addition of His-tag EGFP (3.61 μM) to the SWNT/CHI microarray bearing Ni-NTA, demonstrating additional stepwise fluorescence quenching. (d) Histogram of the rate constants for binding His-tag EGFP to Ni-NTA on SWNT/CHI microarray. (e) Representative fluorescence time-traces (red) for the addition of anti-His-tag antibody (100 nM to 10 pM), showing the clear stepwise fluorescence increase. This stepwise increase response indicates single protein-protein interaction on SWNT. Black line in all traces denotes the fitted trace from Chisquared error-minimizing step-finding algorithm.



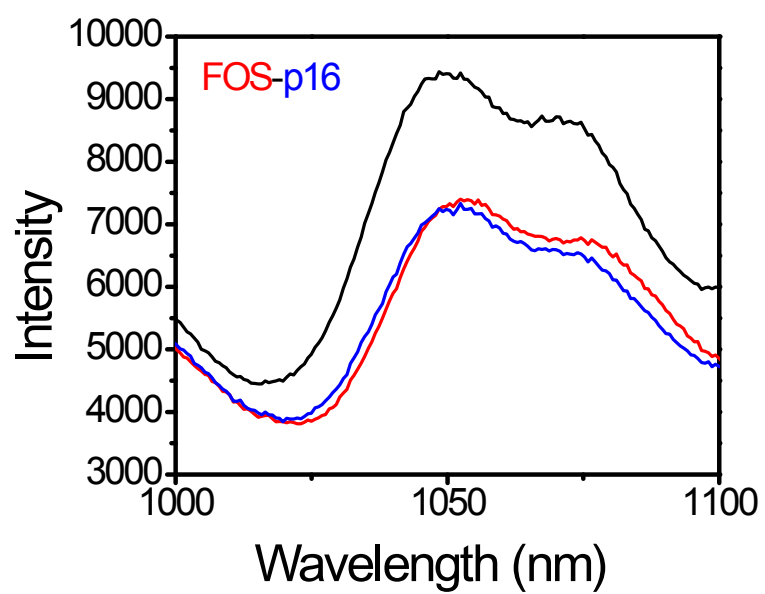
c



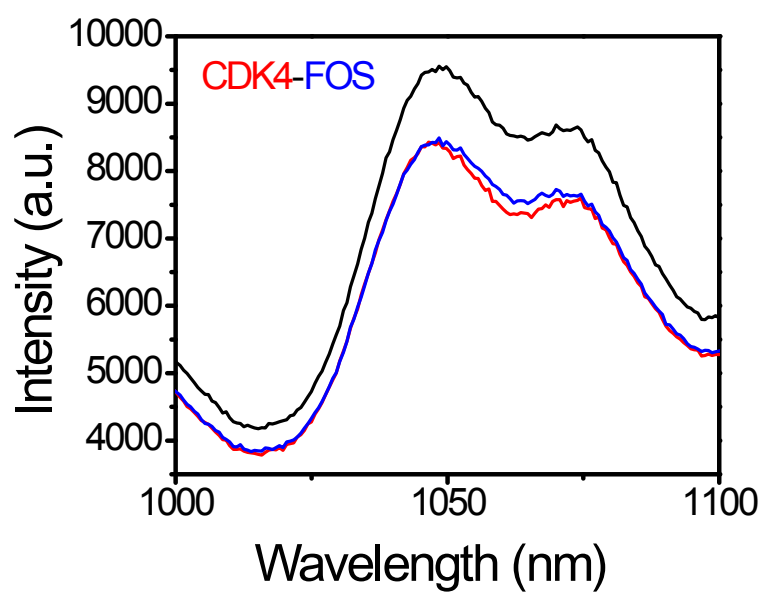
d



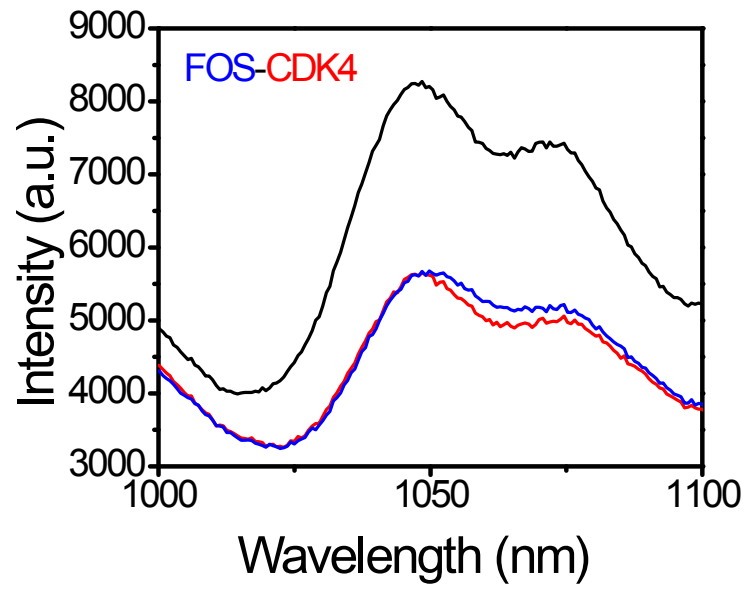
e



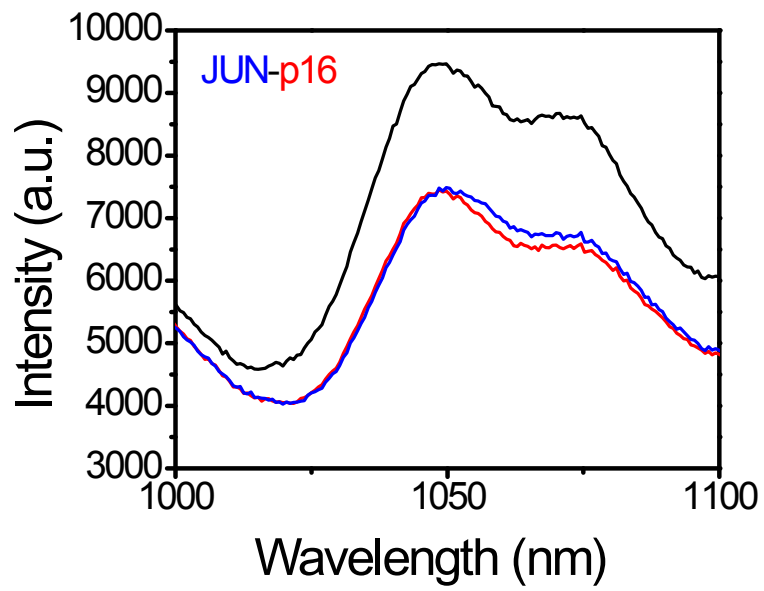
f



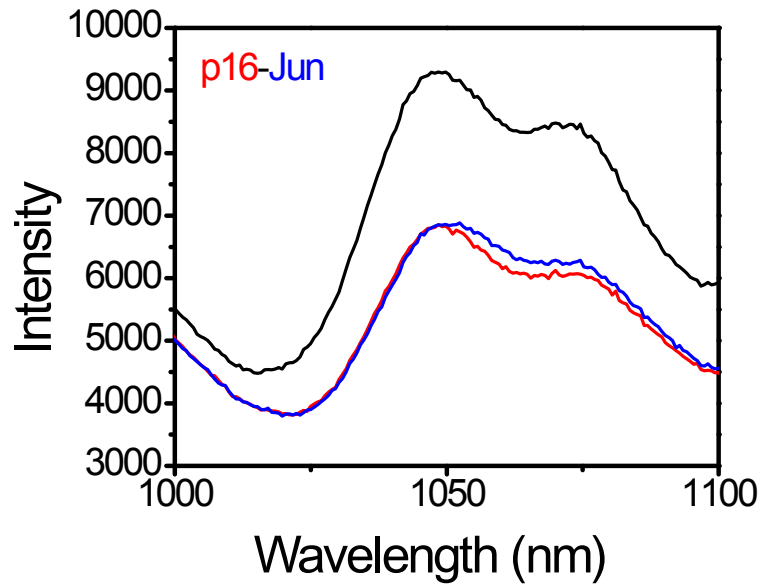
g



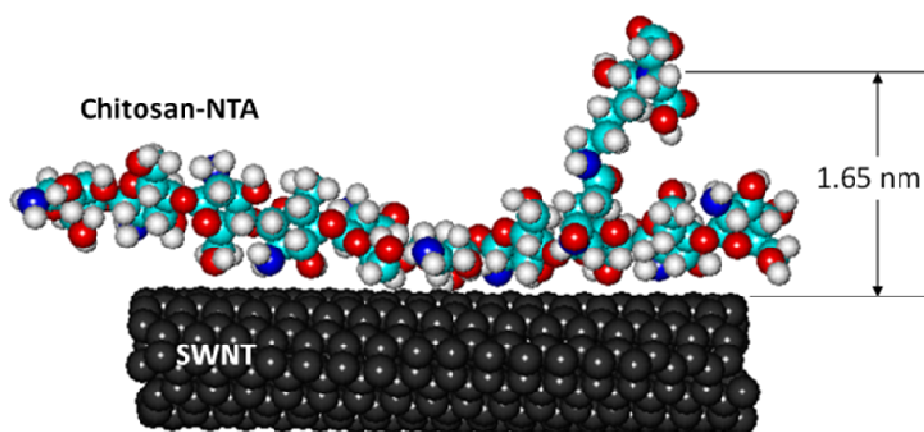
h



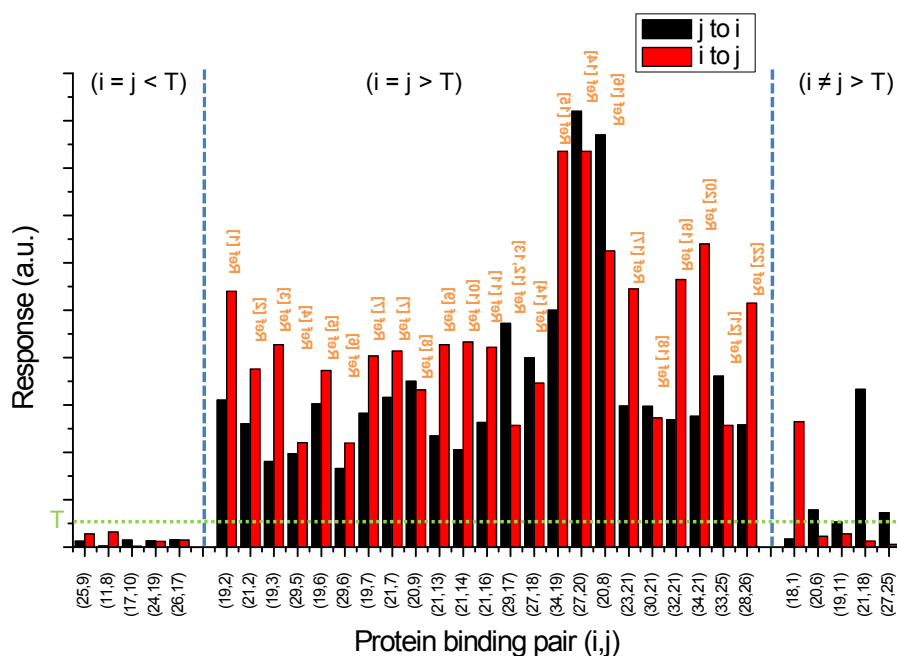
i



Supporting Figure S8. Protein-protein interactions on SWNT/CHI array. nIR fluorescence spectra of SWNT before and after protein addition. Using Jun, Fos, CDK4, and p16 as queries, protein-protein interaction was analyzed by detecting the fluorescence changes. (a) p16-CDK4, (b) FOS-JUN, (c) CDK4-JUN, (d) Jun-CDK4, (e) FOS-p16, (f) CDK4-FOS, (g) FOS-CDK4, (h) JUN-p16, (i) p16-JUN. The first His-tag protein indicated in red was expressed on SWNT/CHI array, and then the second protein without His-tag indicated in blue was added to each well, respectively. Nanotubes were excited at 85 mW with a 785 nm laser.



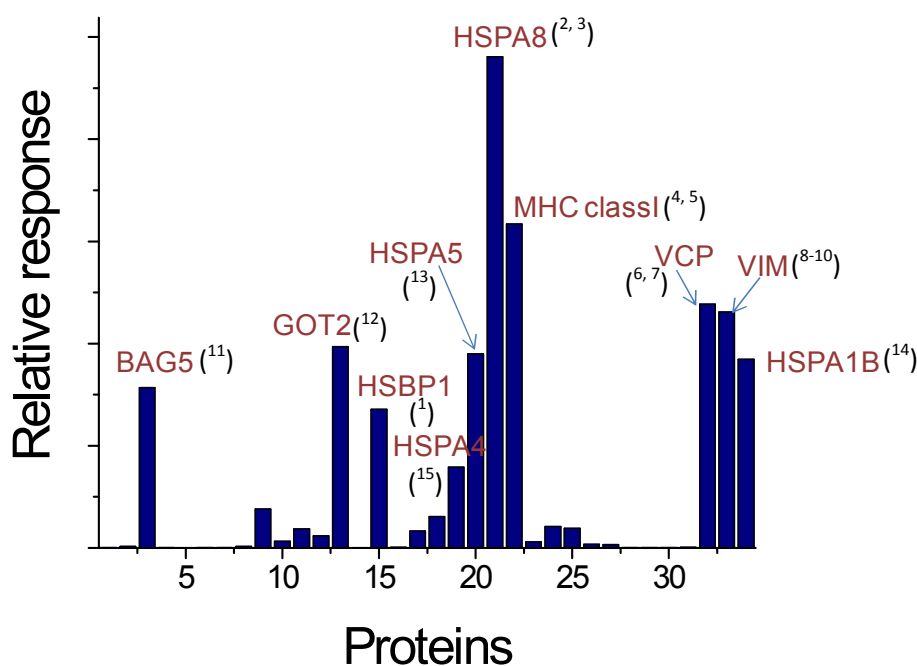
Supporting Figure S9. Distance calculation between the SWNT and Ni-NTA moiety. The distances corresponding to 10 monomer chitosan units and the Ni-NTA moiety were estimated from a Hyperchem molecular model. Geometry optimization was performed in the presence of water at 300K for 1ps providing the shortest possible distance between the SWNT and NTA is 1.65 nm.



Supporting Figure S10. Published literature of protein-protein interaction shown in Figure 5b.

1. Lau, P.P. & Chan, L. Involvement of a chaperone regulator, Bcl2-associated athanogene-4, in apolipoprotein B mRNA editing. *J Biol Chem* **278**, 52988-52996 (2003).
2. Miki, K. & Eddy, E.M. Tumor necrosis factor receptor 1 is an ATPase regulated by silencer of death domain. *Molecular and Cellular Biology* **22**, 2536-2543 (2002).
3. Chung, K.K.K. & Dawson, T.M. Parkin and Hsp70 sacked by BAG5. *Neuron* **44**, 899-901 (2004).
4. Scholz, G.M., Cartledge, K. & Hall, N.E. Identification and characterization of Harc, a novel Hsp90-associating relative of Cdc37. *J Biol Chem* **276**, 30971-30979 (2001).
5. Oh, W.K. & Song, J. Cooperative interaction of Hsp40 and TPR1 with Hsp70 reverses Hsp70-HspBp1 complex formation. *Mol Cells* **16**, 84-91 (2003).
6. Ballinger, C.A. et al. Identification of CHIP, a novel tetratricopeptide repeat-containing protein that interacts with heat shock proteins and negatively regulates chaperone functions. *Molecular and Cellular Biology* **19**, 4535-4545 (1999).
7. Lau, P.P. et al. A DnaJ protein, apobec-1-binding protein-2, modulates apolipoprotein B mRNA editing. *J Biol Chem* **276**, 46445-46452 (2001).
8. Cunnea, P.M. et al. ERdj5, an endoplasmic reticulum (ER)-resident protein containing DnaJ and thioredoxin domains, is expressed in secretory cells or following ER stress. *J Biol Chem* **278**, 1059-1066 (2003).
9. Lain, B., Iriarte, A., Mattingly, J.R., Moreno, J.I. & Martinezcarrion, M. Structural Features of the Precursor to Mitochondrial Aspartate-Aminotransferase Responsible for Binding to Hsp70. *J Biol Chem* **270**, 24732-24739 (1995).
10. Imai, Y. et al. CHIP is associated with Parkin, a gene responsible for familial Parkinson's disease, and enhances its ubiquitin ligase activity. *Mol Cell* **10**, 55-67 (2002).
11. Stocki, P. et al. Identification of potential HLA class I and class II epitope precursors associated with heat shock protein 70 (HSPA). *Cell Stress Chaperon* **15**, 729-741 (2010).
12. Hernandez, M.P., Sullivan, W.P. & Toft, D.O. The assembly and intermolecular properties of the hsp70-Hop-hsp90 molecular chaperone complex. *J Biol Chem* **277**, 38294-38304 (2002).

13. Zhang, L.G., Nephew, K.P. & Gallagher, P.J. Regulation of death-associated protein kinase - Stabilization by HSP90 heterocomplexes. *J Biol Chem* **282**, 11795-11804 (2007).
14. Gramolini, A.O. et al. Sarcolipin retention in the endoplasmic reticulum depends on its C-terminal RSYQY sequence and its interaction with sarco(endo)plasmic Ca²⁺-ATPases. *P Natl Acad Sci USA* **101**, 16807-16812 (2004).
15. Singh, O.V., Pollard, H.B. & Zeitlin, P.L. Chemical rescue of deltaF508-CFTR mimics genetic repair in cystic fibrosis bronchial epithelial cells. *Mol Cell Proteomics* **7**, 1099-1110 (2008).
16. Chevalier, M., Rhee, H., Elguindi, E.C. & Blond, S.Y. Interaction of murine BiP/GRP78 with the DnaJ homologue MTJ1. *J Biol Chem* **275**, 19620-19627 (2000).
17. Imai, Y. et al. A product of the human gene adjacent to parkin is a component of Lewy bodies and suppresses pael receptor-induced cell death. *J Biol Chem* **278**, 51901-51910 (2003).
18. Oh-hashii, K., Naruse, Y., Amaya, F., Shimosato, G. & Tanaka, M. Cloning and characterization of a novel GRP78-binding protein in the rat brain. *J Biol Chem* **278**, 10531-10537 (2003).
19. Vij, N., Fang, S. & Zeitlin, P.L. Selective inhibition of endoplasmic reticulum-associated degradation rescues DeltaF508-cystic fibrosis transmembrane regulator and suppresses interleukin-8 levels: therapeutic implications. *J Biol Chem* **281**, 17369-17378 (2006).
20. Singh, O.V., Pollard, H.B. & Zeitlin, P.L. Chemical rescue of Delta F508-CFTR mimics genetic repair in cystic fibrosis bronchial epithelial cells. *Mol Cell Proteomics* **7**, 1099-1110 (2008).
21. Correia, I., Chu, D., Chou, Y.H., Goldman, R.D. & Matsudaira, P. Integrating the actin and vimentin cytoskeletons: Adhesion-dependent formation of fimbrin-vimentin complexes in macrophages. *J Cell Biol* **146**, 831-842 (1999).
22. Hakimi, M.A. et al. A chromatin remodelling complex that loads cohesin onto human chromosomes. *Nature* **418**, 994-998 (2002).



Supporting Figure S11. Homo-multimer interaction analysis based on literature survey.

1. Liu, X.Q. et al. Crystal structure of the hexamer of human heat shock factor binding protein 1. *Proteins* **75**, 1-11 (2009).
2. Chou, C.C. et al. Crystal structure of the C-terminal 10-kDa subdomain of Hsc70. *J Biol Chem* **278**, 30311-30316 (2003).
3. Gassler, C.S., Wiederkehr, T., Brehmer, D., Bukau, B. & Mayer, M.P. Bag-1M accelerates nucleotide release for human Hsc70 and Hsp70 and can act concentration-dependent as positive and negative cofactor. *J Biol Chem* **276**, 32538-32544 (2001).
4. Ewing, R.M. et al. Large-scale mapping of human protein-protein interactions by mass spectrometry. *Mol Syst Biol* **3**, - (2007).
5. Li, L.O. & Bouvier, M. Structures of HLA-A*1101 complexed with immunodominant nonamer and decamer HIV-1 epitopes clearly reveal the presence of a middle, secondary anchor residue. *J Immunol* **172**, 6175-6184 (2004).
6. Kobayashi, T., Tanaka, K., Inoue, K. & Kakizuka, A. Functional ATPase activity of p97/valosin-containing protein (VCP) is required for the quality control of endoplasmic reticulum in neuronally differentiated mammalian PC12 cells. *J Biol Chem* **277**, 47358-47365 (2002).
7. DeLaBarre, B. & Brunger, A.T. Nucleotide dependent motion and mechanism of action of p97/VCP. *J Mol Biol* **347**, 437-452 (2005).
8. Strelkov, S.V. et al. Conserved segments 1A and 2B of the intermediate filament dimer: their atomic structures and role in filament assembly. *Embo J* **21**, 1255-1266 (2002).
9. Strelkov, S.V. et al. Evolutionarily conserved alpha-helical segments 1A and 2B of the intermediate filament dimer: their atomic structures and role in filament assembly. *Mol Biol Cell* **12**, 54a-55a (2001).

10. Stelzl, U. et al. A human protein-protein interaction network: A resource for annotating the proteome. *Cell* **122**, 957-968 (2005).
11. Kalia, S.K. et al. BAG5 inhibits parkin and enhances dopaminergic neuron degeneration. *Neuron* **44**, 931-945 (2004).
12. Artigues, A., Iriarte, A. & MartinezCarrion, M. Refolding intermediates of acid-unfolded mitochondrial aspartate aminotransferase bind to hsp70. *J Biol Chem* **272**, 16852-16861 (1997).
13. Kuznetsov, G., Chen, L.B. & Nigam, S.K. Several Endoplasmic-Reticulum Stress Proteins, Including Erp72, Interact with Thyroglobulin during Its Maturation. *J Biol Chem* **269**, 22990-22995 (1994).
14. Vos, M.J., Hageman, J., Carra, S. & Kampinga, H.H. Structural and functional diversities between members of the human HSPB, HSPH, HSPA, and DNAJ chaperone families. *Biochemistry-Us* **47**, 7001-7011 (2008).
15. Swain, J.F. et al. Hsp70 chaperone ligands control domain association via an allosteric mechanism mediated by the interdomain linker. *Mol Cell* **26**, 27-39 (2007).